NOVEL PI/ORGANOCLAY NANOCOMPOSITES OBTAINED FROM 2,5-BIS-(AMINOPYRIDINE-2-YL)-1,3,4-OXADIAZOLE (BAPO)

Yagoub Mansoori*, Mina Ghanbary

Department of Applied Chemistry, College of Science, University of Mohaghegh Ardabili, Ardabil, Iran

Abstract

Cation exchange reaction between the hydrochloride salt of 2,5-bis-(aminopyridine-2-yl)-1,3,4-oxadiazole (BAPO) and sodium montmorillonite (Na^{+}-Mt) gave an organophilic clay (BAPO-Mt). The intercalation of BAPO within the clay galleries is confirmed by wide-angle X-ray diffraction (XRD). A series of organoclay/polyimide nanocomposites (CPN) consisting of BAPO and benzophenone-3,3',4,4'-tetracarboxylic dianhydride (BTDA) were also obtained by an in situ polymerization reaction followed by thermal imidization. Structural properties and thermal stability of the obtained CPNs were studied by XRD, TGA, differential scanning calorimetry (DSC), and differential thermal analysis (DTA). XRD patterns showed that CPNs 1-3wt.% may have exfoliated structure while in the CPN 5wt.% intercalated structure is significant. The glass transition temperature (T_g) is increased with respect to pristine PI for CPNs 1-3wt.%. Based on the obtained results, CPN 1wt.% showed the most improved thermal properties. Single electron microscopy (SEM) showed that the film obtained from CPN 1wt.% has smoother surface than that of pristine PI.

Key words: *nanocomposite, clay modification, montmorillonite, polyimide, layered silicate*

1. INTRODUCTION

Polyimides (PI) have gained interests in both academia and industries due to their excellent thermal stability, good resistance toward organic solvents, and improved mechanical properties (Wang et al., 2012). They have been applied widely in the areas of modern industries (Imai et al., 2002). These super engineering plastics have found their way into aerospace (Meador et al., 2012), electrical/electronic applications (Nguyen et al., 2007), gas separation (Chatzidaki et al., 2007), biochip design (Matsumoto et al., 2008), coating, and composites (Köytepe et al., 2008, Mansoori et al., 2011a).

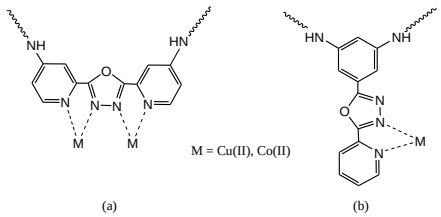
However, some difficulties come from rigidity and poor solubility in processing of most PIs. Introduction of flexible linkages between the aromatic rings of the main chain is an effective way to make these polymers more pliable (Ebadi and Mehdipour-Ataei, 2010, Mehdipour-Ataei and Zigheimat, 2007, Mansoori et al., 2011c). It was also shown that, the incorporation of rigid heterocyclic rings in the main chain of a synthetic polymer could provide excellent thermal and thermo-oxidative stability, which should be useful to decrease negative effects resulting from the introduction of flexible linkages mentioned above. Pyridine nucleolus, as a rigid symmetric aromatic ring, would contribute to the thermal stability, chemical stability, and retention of mechanical property of the resulting polymer at elevated temperature. Furthermore, the polarizability, resulting from the nitrogen atom in the pyridine ring, could be suitable to improve their solubility in organic solvents (Wang et al., 2009). Fujigaya et al. reported among the variety of polybenzimidazole derivatives, the pyridine-containing polymer is known to possess a better mechanical properties and significantly higher proton conductivity due to its higher acid doping ability (Fujigaya et al., 2009).

On the other hand, it was known that, the thermal stability of polymers can be raised by the incorporation of 1,3,4-oxadiazole moieties into the polymer structure (Ding et al., 2002). The outstanding thermal stability is ascribed to the electronic equivalency of the oxadiazole ring to the phenylene ring structure, which has high thermal-resistance (Souza et al., 2004).

Combination of inorganic materials with organic polymers is one the exciting topics that has been receiving increasing research attention during recent decades. Nanostructured hybrid materials showed

wide potential applications in various areas such as in coatings (Voevodin et al., 1999), catalysis (Ringwald and Pemberton, 1999) and biotechnology (Yokoyama et al., 2006), shape memory polymers (Yoonessi et al., 2012), and fuel cells (Battirola et al., 2012). Organically modified clays have improved compatibility, hence higher efficiency of reinforcement, with the polymer matrix. It has been known that, the dispersion of small amounts reinforcing organoclay mineral with high-aspect ratios, such as layered silicate clays, can significantly enhance the properties of PI and its precursor poly(amic acid) (PAA). These improvements can include solvent resistance (Burnside and Giannelis, 1995), ionic conductivity (Vaia et al., 1995), enhanced fire retardance (Gilman et al., 2000b), increased corrosion protection (Yeh et al., 2004b), increased strength and heat resistance (Long et al., 2007), decreased gas permeability (Zhong et al., 2007), high moduli (Liu, 2007), and dielectric properties (Yeum, 2011). The enhancements in thermal and mechanical properties of CPNs are due to the lamellar structure of montmorillonite those results in high in-plane strength and stiffness, and a high aspect ratio (Huang et al., 2008). In addition, clay is a reinforcing material, naturally abundant, nontoxic, inexpensive, chemically and thermally stable (Tunç et al., 2012). The chemical structure of Na^{+}-Mt consists of two fused silica tetrahedral sheets sandwich an edge-shared octahedral sheet of either aluminum or magnesium hydroxide (Sinha Ray and Okamoto, 2003). The Ca^{2+} and Na^{+} ions adsorbed in the interlayer region are exchangeable with organic cations such as long chain alkyl ammonium (Wang et al., 2007a). These organoclays may be suitable for polymer blends prepared with a low processing temperature. They have low thermal stability and their decomposition occur around 200°C, whereas the melt-processing temperatures of most polymers are typically above 200°C (Liaw et al., 1998). Furthermore, the preparation and processing of PI/organoclay nanocomposites is carried out at high temperatures, and the pyrolysis of the long carbon chain of quaternary ammonium salts is inevitable. In addition, thermal decomposition during processing can initiate/catalyze polymer degradation, in addition to a variety of undesirable effects during processing and in the final product (Yousfi et al., 2013, Yeh et al., 2004a). To avoid the detrimental effects, modification of clay minerals with imidazolium (Sheng et al., 2012) and phosphonium (Abdallah and Yilmazer, 2013) salts have been noted. As another approach, using of aromatic amines and/or diamines, as swelling agents, has also been considered in the preparation of polyamide and polyimide (PI) nanocomposites (Huang et al., 2008, Mansoori and Darvishi, 2014, Mansoori and Mohseni Masooleh, 2015).

Recently, we reported the synthesis of a new aromatic diamine, 2-(5-(3,5-diaminophenyl)-1,3,4-oxadiazole-2-yl)pyridine (POBD). Thermally stable polyamides (Mansoori et al., 2012b), polyimides (Mansoori et al., 2012a), and PI/Clay nanocomposites (Mansoori et al., 2013) have been prepared using POBD. We noticed to the metal coordination ability of the 1,3,4-oxadiazole ring adjacent to 2-pyridyl group in designing POBD. The ability of prepared hybrid materials for removal of the Co(II) ion have also been investigated (Mansoori et al., 2011b). As a part of our continuing efforts on the synthesis of polymers with high thermal stability and metal ions coordination ability of higher capacity, we recently reported the synthesis and characterization of another designed aromatic monomer containing pyridine and 1,3,4-oxadiazole moieties, BAPO (Mansoori and Mohsenzadeh, 2015, Mansoori and Ghanbari, 2015) Based on our results, the polyamides obtained from BAPO show higher absorption capacity toward metal ions than those PIs obtained from POBD (Mansoori and Mohsenzadeh, 2015) This can be attributed to the fact that the numbers of coordination sites in BAPO are higher than that of POBD, Scheme 1.



Scheme 1. Proposed structure for the coordination of metal ions toward a polyamide obtained from: (a) BAPO; and (b) POBD (Mansoori and Mohsenzadeh, 2015).

In this work, the dihydrochloride salt of BAPO was used as a swelling agent for the treatment of Na^{+}-Mt. The novel modified organoclay (BAPO-Mt) was used in the preparation of PI/organoclay hybrids of BAPO/BTDA. Thermal stability of BAPO is higher than those for commonly used quaternary alkyl ammonium salts. Therefore, thermal degradation will be prevented during heat treatment needed for curing of poly(amic acid). The obtained films were studied by FT-IR spectroscopy, XRD, and SEM. The thermal properties were examined by thermo-gravimetric analysis-differential thermal analysis (TGA-DTA) and DSC.

2. EXPERIMENTAL

2.1. Instruments

The FT-IR (KBr) spectra were recorded on a PerkinElmer RXI spectrophotometer (USA). NMR spectra were obtained on a Bruker 300 MHz spectrophotometer (USA). DSC and TGA thermograms were measured on Mettler Toledo DSC-1 (USA) and Linseis STA PT 1000 (France) instruments, respectively. Elemental analyses of the samples were performed on an Elementar Vario EL III instrument (Germany). XRD measurements were performed at room temperature on a Simence D500 X-ray diffractometer (Germany) using Ni-filtered Cu-K_α radiation. The scanning rate was 1°/min over a range of 2θ = 2-10°. Inherent viscosities were measured by an Ostwald viscometer at 25°C in DMSO. Scanning Electron Microphotographs were obtained on a LEO 1430VP instrument (UK).

2.2 Material

All chemicals solvents were laboratory grade and were obtained from Merck (Germany). All solvents were dried according to procedures described in the literature (Armarego and Chai, 2009). 6-Aminopicolinic acid **4** was prepared according to the method described in literature in three steps starting from 6-amino-2-methylpyridine **1** in overall 36.9% yield (Fukase et al., 1994).

2.2.1 Synthesis of 2,5-bis-(aminopyridine-2-yl)-1,3,4-oxadiazole, BAPO **5**

The diamine, BAPO, was synthesized under anhydrous condition according to the method described earlier (Mansoori and Ghanbari, 2015). To the stirred solution of 6-aminopicolinic acid (1.380 g, 0.01 mole) and hydrazine sulfate (0.650 g, 0.005 mole) in concentrated phosphoric acid (85%, 2.8 ml), P_2O_5 (4.260 g, 0.03 mole) was added slowly followed by addition of $POCl_3$ (0.9 ml, 0.01 mole). The viscous solution was heated at 160°C for 2h while magnetic stirring. After cooling to room temperature, the reaction mixture was poured over crushed ice with vigorous stirring. The mixture was neutralized with 10% sodium hydroxide solution to pH=6, then completely neutralized with 5% solution of sodium hydrogen carbonate and filtered in vacuum. The precipitate was then stirred in 10 ml of distilled water for 30 min, filtered in vacuum and then dried, to give 0.670 g (53.0% yield) of a pale yellow solid product. mp = 273-275°C (272.9°C, measured by DTA). FT-IR (KBr, cm^{-1}): 3377 (m), 3332 (m), 3202 (s), 3096 (w), 1653 (w), 1603 (w), 1575 (m), 1273 (m). ^{1}H NMR (300 MHz, DMSO-d_6, δ, ppm): 7.51, (br,s 2H, ArH), 7.27 (br,s 2H, ArH), 6.60 (br,s 2H, ArH), 6.32 (br,s 4H, NH_2, exchanged with D_2O), 3.45 (br, s, H_2O). ^{13}C NMR (75 MHz, DMSO-d_6, δ, ppm): 164.7, 160.4, 141.2, 138.5, 111.8, 111.7. Mass: $(m/e)^+$: 254 (100%).

2.2.2 Preparation of the polyimide film

To a solution of BAPO (0.1589 g, 0.625 mmol) in 2.5 ml of DMSO, BDTA (0.2013 g, 0.625 mmol) was gradually added. The mixture was stirred at room temperature for 6 h under argon. The obtained DMSO solution of PAA was poured onto a glass plate, and then heated from 60 to 270ºC (at a heating rate of 1 ºC/min) in a furnace. The film was then peeled off from the glass plate to obtain the PI film (90.6 % yields). FT-IR (KBr, cm^{-1}): 1786 (m), 1727 (m), 1673 (w), 1366 (m), 1094 (s), 722 (s). Found (%): C 62.60; H 3.02; N 15.57. $(C_{29}H_{12}N_6O_6)_n$. Calculated (%): C 64.45; H 2.24; N 15.55.

2.2.3. Preparation of the organophilic clay, BAPO-Mt

Na^{+}-Mt (2.000 g) was stirred in 100 ml of distilled water (beaker A) at room temperature overnight. A separate solution containing BAPO (2.22 mmol) in 70 ml of distilled water (beaker B) was kept under magnetic stirring at 80°C and then 35% aqueous HCl was added to adjust the pH value to about 3-4. After complete dissolution of diamine, the contents of beaker A were added under vigorous stirring and then stirred at 80°C for an hour. The organoclay was filtered in a Buchner funnel. To remove any excess ammonium ions, the precipitate was washed with distilled hot water until a chloride ion test with a 0.1 M $AgNO_3$ solution was negative and then dried in vacuum at 50°C for 48 h (Wang et al., 2007b).

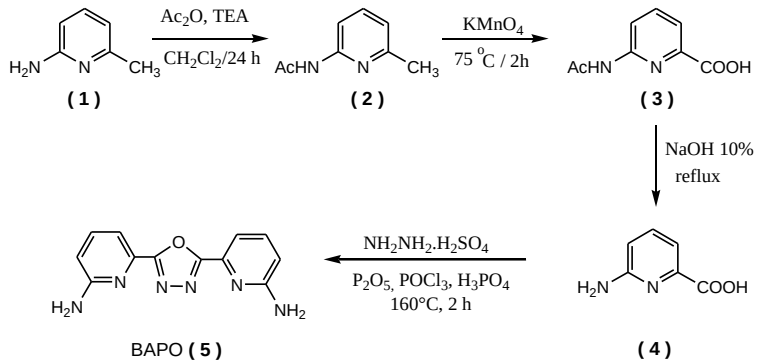
2.2.4. Preparation of the CPN films

The preparation CPNs were carried out through a thermal imidization reaction of PAA/BAPO-Mt dispersion in DMSO according to the method described earlier (Mansoori et al., 2011b, Mansoori et al., 2013). A typical procedure to prepare a hybrid film containing 1wt.% of BAPO-Mt is described as follows: BAPO-Mt (3.04 mg) was magnetically stirred vigorously at room temperature for 24 h in 3 ml of DMSO to yield a DMSO dispersion of BAPO-Mt (beaker A). A separate solution was prepared by dissolving BAPO (0.1589 g, 0.625 mmol) in 2 ml of DMSO under magnetic stirring for 10 min at room temperature (beaker B). The contents of the beaker B were added to beaker A and stirred vigorously for another 24 h at room temperature. Then, a solution of BTDA (0.2019 g, 0.626 mmol) in 2 ml of DMSO was prepared under magnetic stirring for 10 min at room temperature (beaker C). Beaker C was then added to beaker A+B and the contents were stirred for an additional 24 h at room temperature to yield a DMSO solution of PAA/organoclay. The mixture was poured on a glass plate, allowed to stand at room temperature overnight, and then heated from 60 to 270ºC (at a heating rate of 1ºC/min) in a high temperature oven. The film was then peeled off from the glass plate to obtain the PI/organoclay hybrid film.

3. RESULTS AND DISCUSSION

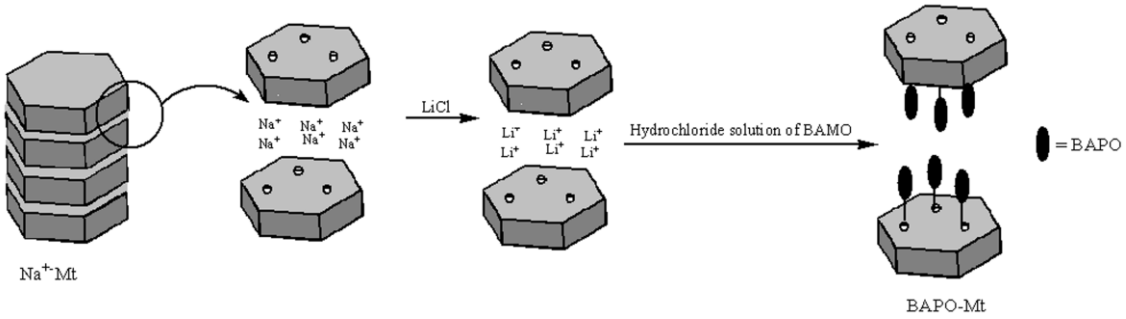
3.1. Preparation of BAPO-modified organoclay

The diamine, BAPO, was synthesized in four steps in overall 20.0% yield (Mansoori and Ghanbari, 2015). At first step, 2-amino-6-methtypyridine was acetylated with acetic anhydride, oxidized with potassium permanganate in second step and then alkaline hydrolyzed to give 6-amino-picolinic acid in third step (Fukase et al., 1994). In the last step, cyclo-dehydration of **4** with hydrazine sulfate in the presence of P_2O_5 in the mixture of $POCl_3$ and concentrated phosphoric acid gave BAPO (Scheme 2).



Scheme 2. Synthesis of BAPO

To prepare the organophilic clay (BAPO-Mt) via a cation exchange reaction, Na^{+}-Mt was initially mixed with a hydrochloride solution of BAPO **5**, Scheme 3.



Scheme 3. Modification of Na^{+}-Mt with BAPO.

3.2. Characterization of BAPO-Mt organoclay

Figure 1 shows FT-IR spectra of BAPO, sodium montmorillonite, and BAPO-Mt. The spectrum of organoclay exhibits the characteristic bands of Mt and BAPO: N–H stretching at 3373 and 3206 cm^{-1}, –C=N– stretching of the oxadiazole nucleolus at 1679 cm^{-1}, –C=N– stretching of the pyridine ring at 1575 cm^{-1}, stretching vibrations of the double bonds of the aromatic rings in BAPO at 1627 cm^{-1}, and typical bands of montmorillonite at 1033 and 525 cm^{-1}.

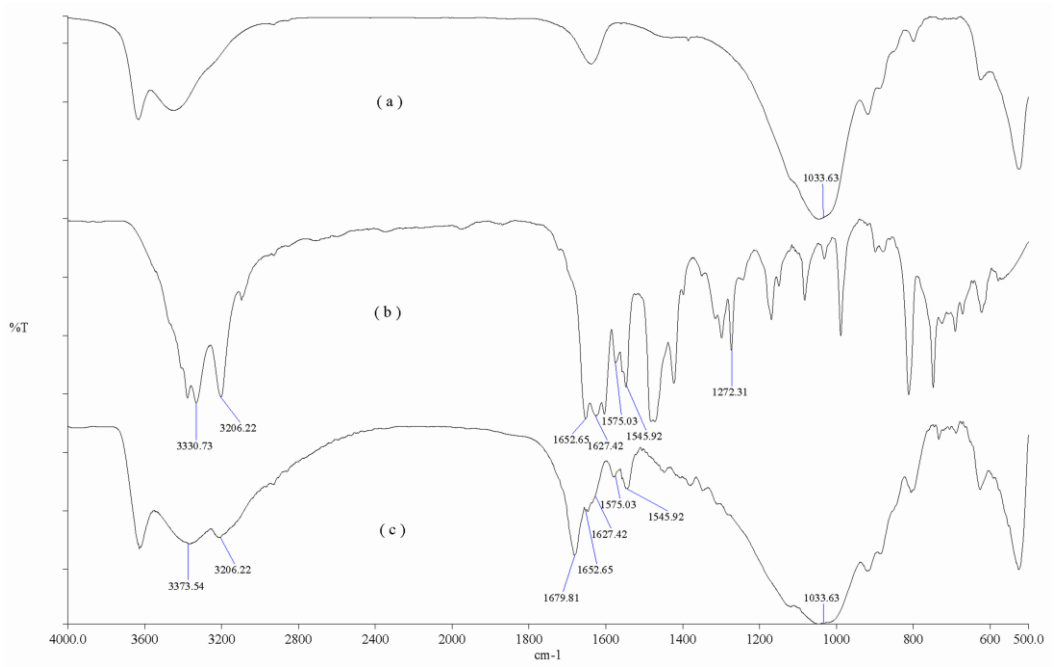


Figure 1. IR spectrum (KBr) of: a) Na^{+}-Mt, b) BAPO, and c) BAPO-Mt.

Figure 2 presents XRD pattern of BAPO-Mt and pristine clay. A strong peak is observed at $2\theta = 8.95°$ for Na^{+}-Mt, corresponding to the (001) plane, indicating that the interlayer spacing (d_{001}-spacing) of Na^{+}-Mt is about 1.0 nm. The interlayer d_{001}-spacing can be calculated from peak positions using Bragg's law: $n\lambda = 2d \sin \theta$, where λ is the X-ray wavelength (1.5418 Å). The reflection peak of (001) in BAPO-Mt shifted to a lower diffraction angle at 6.90°, corresponding to the larger d_{001}-spacing

(1.28 nm) than Na^{+}-Mt. The replacement of sodium ions with the ammonium ions of BAPO seems to increase the d_{001}-spacing of layered silicate. In general, a larger d_{001}-spacing should assist the intercalation of the polymer chains and should also lead to better clay dispersion within the polymer matrix. Table 1 summarizes the diffraction peaks and the calculated d_{001}-spacings of Na^{+}-Mt and BAPO-Mt.

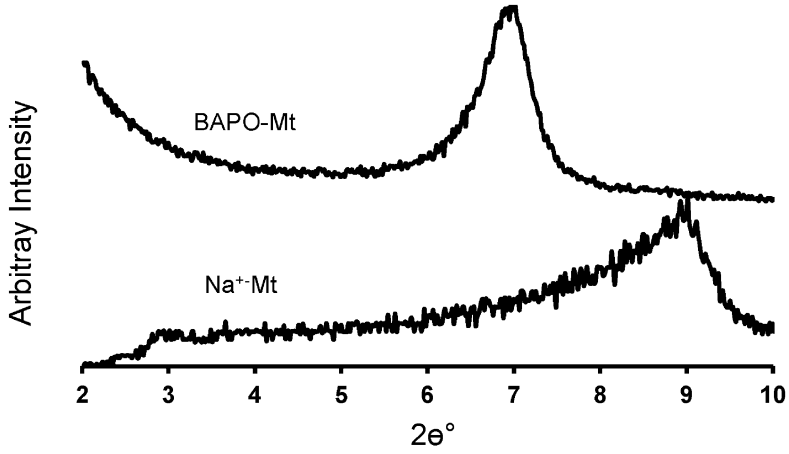


Figure 2. XRD pattern of Na^{+}-Mt and BAPO-Mt.

Table 1. Diffraction peaks and basal spacing of Na^{+}-Mt and BAPO-Mt.

Product	**Diffraction peak and basal spacing**	
	Typical diffraction peak (°)	**Basal spacing (nm)**
Na^{+}-Mt	8.95	1.00
BAPO-Mt	6.90	1.28

The thermal treatment of pristine clay under nitrogen consists of two main stages. The first stage occurs from ambient temperature to 200°C. In this step, free water molecules physically adsorbed on the external surfaces of crystals along with the hydrating water molecules around the exchangeable cations located inside the interlayer space are removed. The second stage is attributed to the dehydroxylation of the structural silanol units of the montmorillonite in the range of 200-700°C. The temperature intervals of dehydration corresponding to these processes as well as the amount of water released depends on the nature of adsorbed cations and the hydration of the surface (Balek et al., 2006). On the other hand, organically modified montmorillonite shows a four-step decomposition process. The vaporization of free water takes place at temperatures below 200°C, while the surfactant's decomposition occurs in the temperature range of 200–500°C. Dehydroxylation of the structural silanol groups related to aluminosilicates occurs between 500–800°C. The last step is the decomposition associated with the combustion reaction between organic carbon and inorganic oxygen (Zidelkheir and Abdelgoad, 2008). The amount of loaded diamine can be estimated by TGA measurement. Figure 3 shows the TGA curves of the Na^{+}-Mt, the BAPO-Mt, and BAPO.

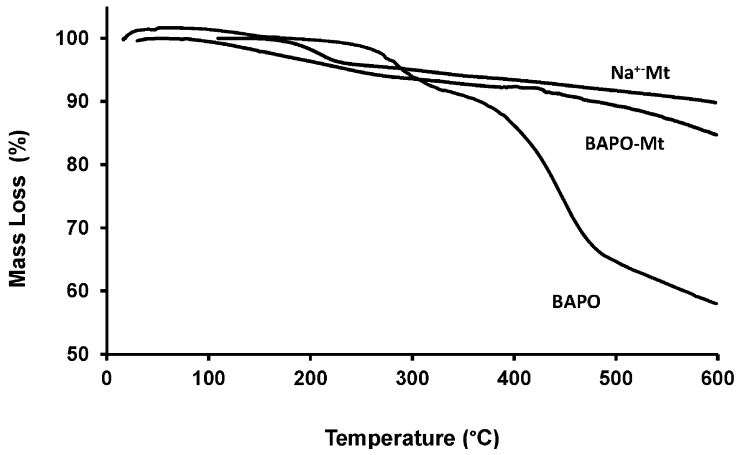


Figure 3. TGA curve (N_2 atmosphere, scan rate of 10°C/min) of Na^{+}-Mt, BAPO-Mt, and BAPO.

Pristine Na^{+}-Mt contains a large quantity of water due to the intercalation of hydrated sodium (Na^{+}) and hydrated calcium (Ca^{2+}) cations inside the clay layers. These physically adsorbed water molecules are removed in the range from ambient temperature to 230°C (ca. 3.81% mass loss). The virgin clay also undergoes a 6.36% mass loss within 230-598°C related to dehydroxylation of the structural silanol units. Whereas, under the same condition BAPO-Mt shows a mass loss of about 10.6% within 230-598°C related to surface dehydroxylation and thermal decomposition of the surfactant molecules within the organoclay galleries. Surface energy of Na^{+}-Mt is lowered by the presence of the aromatic ammonium ions within the interlayer spacing. Therefore, the hydrophilic silicate surface transforms to an organophilic one. The difference between mass losses of Na^{+}-Mt and BAPO-Mt within 230-598°C ($\Delta m = 4.24\%$) can be attributed to the mass of the loaded diamine. The amount of loaded diamines (42.4 mg/g of clay) can be calculated from Eq. (1).

$$Loaded \quad amount \quad (mg/g) = \frac{\Delta m}{100} \times 1000 \qquad Eq.1$$

As seen in Figure 3, the thermal decomposition of the surfactant molecules occurs in two stags at 260°C and 370°C. These temperatures are higher than those of decomposition temperature of aliphatic long chain surfactants commonly used for modification of Na^{+}-Mt, which occurs below 200°C (Liang et al., 2003). This study suggests that the BAPO-Mt can be used in the preparation of PI nanocomposites that need to be cured at elevated temperatures.

The images obtained by SEM demonstrate significant changes on the surface of the BAPO-Mt. The Na^{+}-Mt particles seem to be stuck together due to moisture (Figure 4a-b), but the organoclay particles are clearly separated in organically modified clay (Figure 4c,d). It seems that the hydrophilicity of the clay is reduced after modification reaction. This study is in accordance with TGA results.

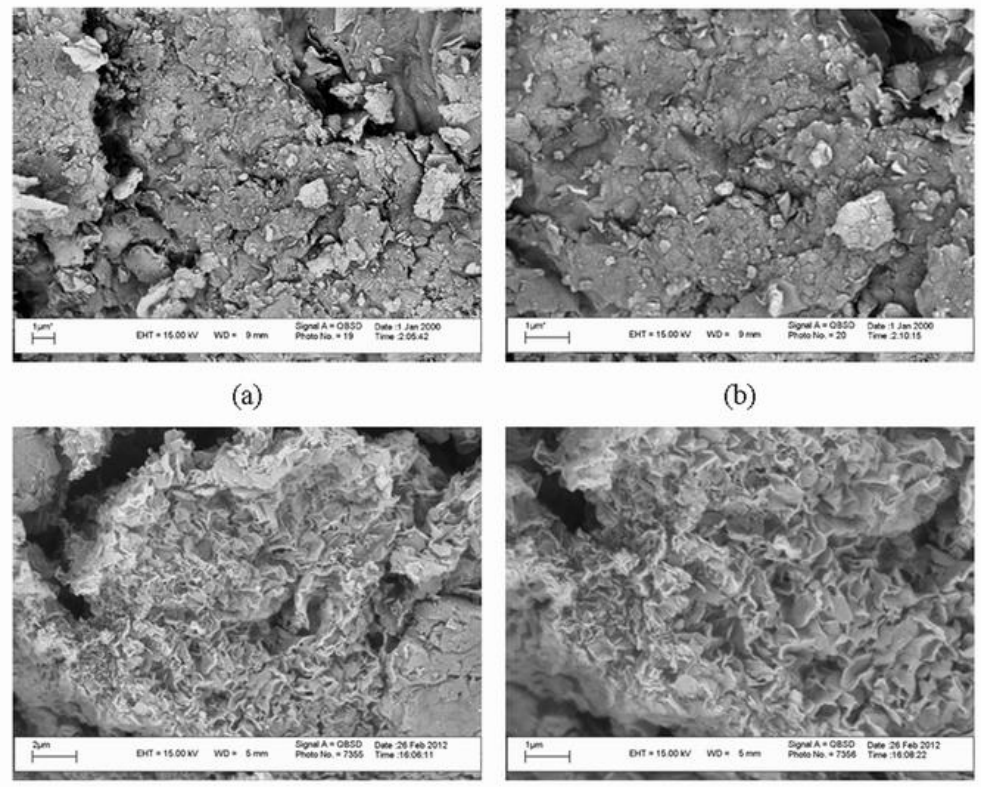
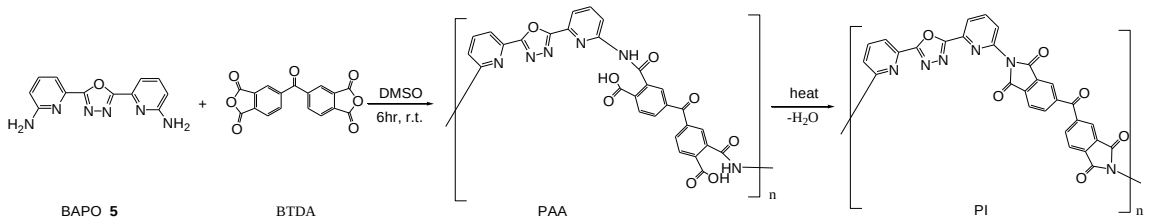


Figure 4. SEM images of Na^{+}-Mt at a) 15000x and b) 30000x; and of BAPO-Mt at c) 15000x and d) 30000x magnifications.

3.3. Polymer Synthesis

Scheme 4 depicts the synthesis of the PI from the reaction of BAPO and BTDA through thermal dehydration of the PAA intermediate.



Scheme 4. Synthesis of the PI.

The FT-IR absorptions appearing at approximately 1786, 1727, 1366, 1094 and 722 cm^{-1} (Figure 5) indicate the presence of imide functional groups in the polyimide film (Le et al., 2012).

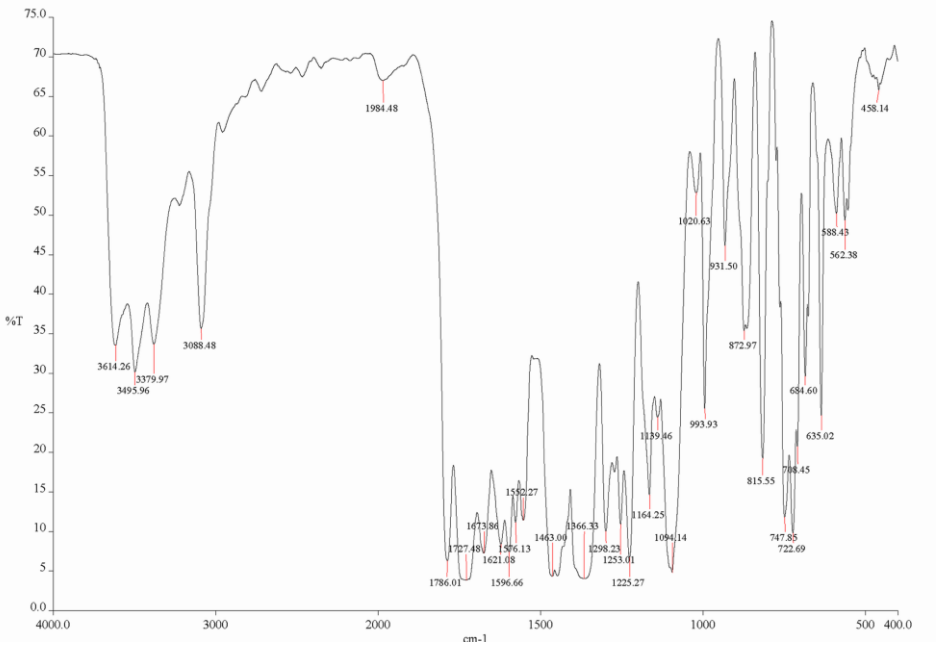


Figure 5. FTIR spectra (thin film) of the PI.

The polyimide is also characterized by elemental analysis. The observed and calculated values for elemental analyses are in good agreement. Solubility test results (Table 2) show that the obtained PI is soluble in dimethylsulfoxide (DMSO) and concentrated sulfuric acid at room temperature as well as in boiling temperature of other polar aprotic solvents such as, dimethylacetamide (DMAc) and N-methylpyrrolidone (NMP). For this experiment, about 0.01 g of the polymer sample was examined in 1 ml of solvent at room and at boiling temperature of the solvents. The inherent viscosity of the 0.125 and 0.25 g/dL solutions of the polyimide were 0.39 and 0.36 dL/g, respectively (measured at 25± 0.5°C in DMSO).

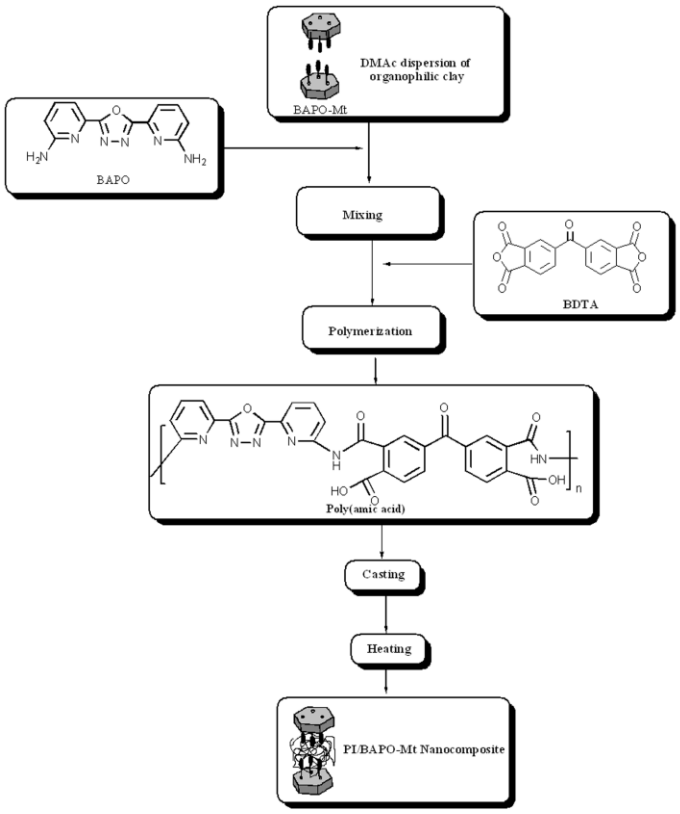
Table 2. Solubility of the PI.

Solvent		DMSO	DMF	DMAc	NMP	MeOH	$CHCl_3$	Acetone	H_2SO_4
PI	R.T.	++[a]	--[b]	+-[c]	+-	--	--	--	++
	Δ[d]	++	+-	++	++	--	--	--	++

[a] Soluble. [b] Insoluble. [c] Partially soluble. [d] Boling temperature of the solvent.

3.4. Preparation and characterization of PI/BAPO-Mt CPNs

The present work reports the preparation and characterization of new polyimide CPNs with different concentrations of BAPO-Mt. Scheme 5 shows a procedure for the preparation of PI/BAPO-Mt CPNs by thermal imidization according to method described earlier (Mansoori et al., 2011b, Mansoori et al., 2013).



Scheme 5. Preparation of PI/BAPO-Mt CPNs by thermal imidization.

Figure 6 presents XRD curves of BAPO-Mt, and PI films with various organoclay contents. The lack of any diffraction peak in the XRD patterns of CPNs 1 and 3wt.%, at 2θ = 2-10°, can be attributed to the possible formation of nanocomposites of exfoliated structure.

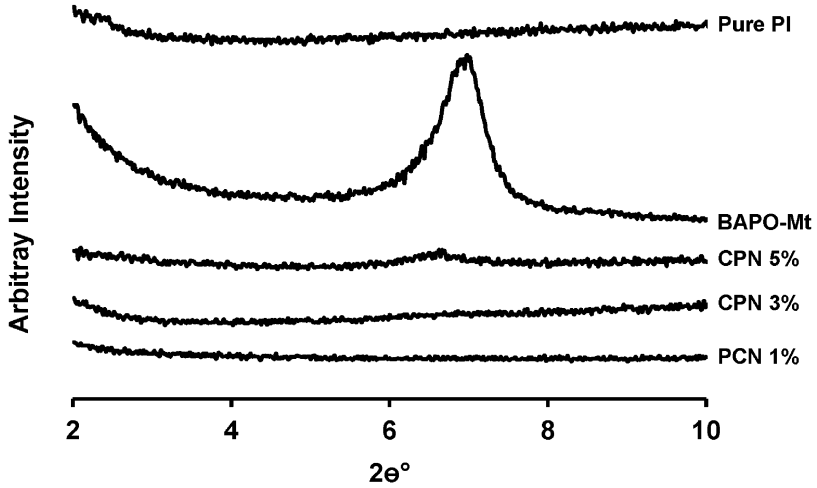


Figure 6. XRD patterns of BAPO-Mt, PI, and PI/BAPO-Mt nanocomposites.

A wide and week diffraction peak at 2θ = 6.62° was displayed by CPN 5wt.%, equaling a d_{001}-spacing of 1.33 nm for the layered silicates in the CPN. The shift to higher interlayer d_{001}-spacing with respect to BAPO-Mt (2θ = 6.90°, d_{001} = 1.28 nm) is due to the intercalation of the polymer within the

organoclay galleries and the formation of an intercalated nanocomposite. Pure polyimide does not show any diffraction peak at 2θ = 2-10°. The XRD data are summarized in Table 3.

Table 3. Diffraction peaks and basal spacing of the PI and CPNs.

Product	Diffraction peak and basal spacing	
	Typical diffraction peak (°)	Basal spacing (nm)
PI	-	-
CPN 1%	-	-
CPN 3%	-	-
CPN 5%	6.62	1.33

The glass transition temperature of the pure PI is observed at about 271.3°C (measured by DSC), and the polymer does not show any melting endotherm. The decomposition of the polymer begins at 435.5°C, and no thermal decomposition occurs below this temperature. To remove any adsorbed water, the polymer samples were heated to 150°C and then cooled to room temperature prior DSC measurements. Figure 7 shows DSC curves related to the PI and CPNs. The results are summarized in Table 4.

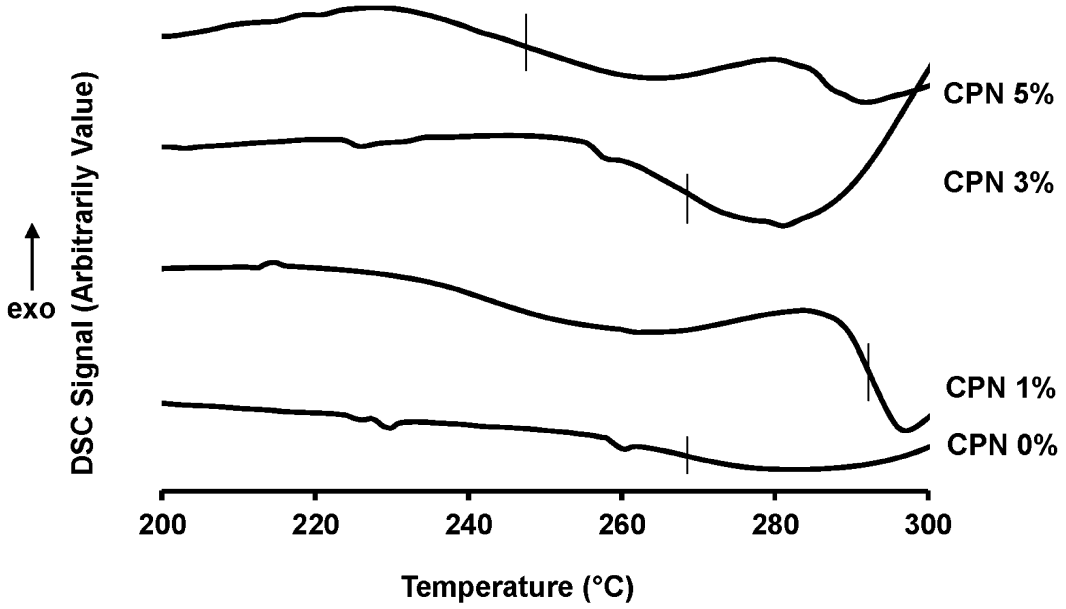


Figure 7. DSC curves of PI and PI/BAPO-Mt with various organoclay contents (N_2 atmosphere, scan rate 10°C/min).

As seen, the glass transition temperature increases dramatically from 271.3°C for pure PI to 297.0°C for CPN 1wt.%. The restriction of the intercalated polymer chains within the clay galleries can be responsible for preventing segmental motions of the polymer chains (Yeh et al., 2004b). However, further addition of organoclay up to 5wt.% leads to a decrease in T_g. This decrease might be due to the aggregation of BAPO-Mt particles that reduces the interfacial interaction between organoclay and the PI matrix (Sinha Ray and Okamoto, 2003). Both DSC and DTA methods show similar trends of changing in the T_g values upon increasing the organoclay content.

Figure 8 shows TGA curves of the pure PI and CPNs. The results are given in Table 4. As seen thermo-gravimetery parameters such as temperature for %10 mass loss and initial thermal decomposition (T_D) are increased for CPN 1wt.%, remained almost unchanged in CPN 3wt.%, and then decreased.

Table 4. Thermal properties of the PI and CPNs.

Polymer	T_g (°C) [a]	%10 Mass loss (°C)	T_D (°C) [b]	Char Yield [c]
PI	271.3 (300.1)	476.0	435.6	67.95
CPN 1%	297.0 (326.7)	479.1	443.5	66.85
CPN 3%	269.3 (300.4)	484.8	444.4	68.25
CPN 5%	248.5 (295.5)	482.8	436.1	68.67

[a] Obtained based on DSC measurements. The values in the parentheses were obtained based on DTA measurements. [b] Onset decomposition temperature. [c] At 599°C.

Char yields are less influenced by the BAPO-Mt content. The drop in the thermal properties at high organoclay loading may be attributed to the better miscibility of polymer and organoclay phases at low organoclay concentrations. Like a superior insulator, the obtained multilayered carbonaceous silicate structure increase the total path of evaporation for small molecules produced during pyrolysis (Gilman et al., 2000a). Based on DSC, DTA and TGA studies, it can conclude that CPN 1wt.% has the most improved thermal properties.

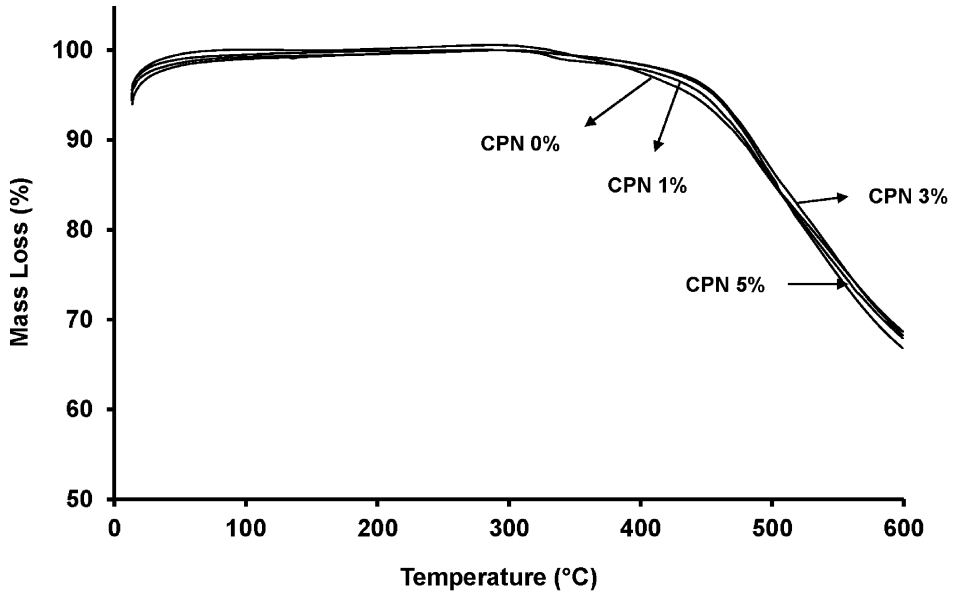


Figure 8. TGA Curves of PI and PI/BAPO-Mt with various organoclay contents (N_2 atmosphere, scan rate 10°C/min).

The morphology of the PI and CPN film surfaces was also studied by SEM. Some significant and interesting changes have been observed in the surface of CPN 1wt.% with respect to virgin PI film, Figures 9a-d. As seen in the pictures, too many micro-cracks are observed in the background of both films, however, surface homogeneity of the film is increased in the CPN 1wt.%.

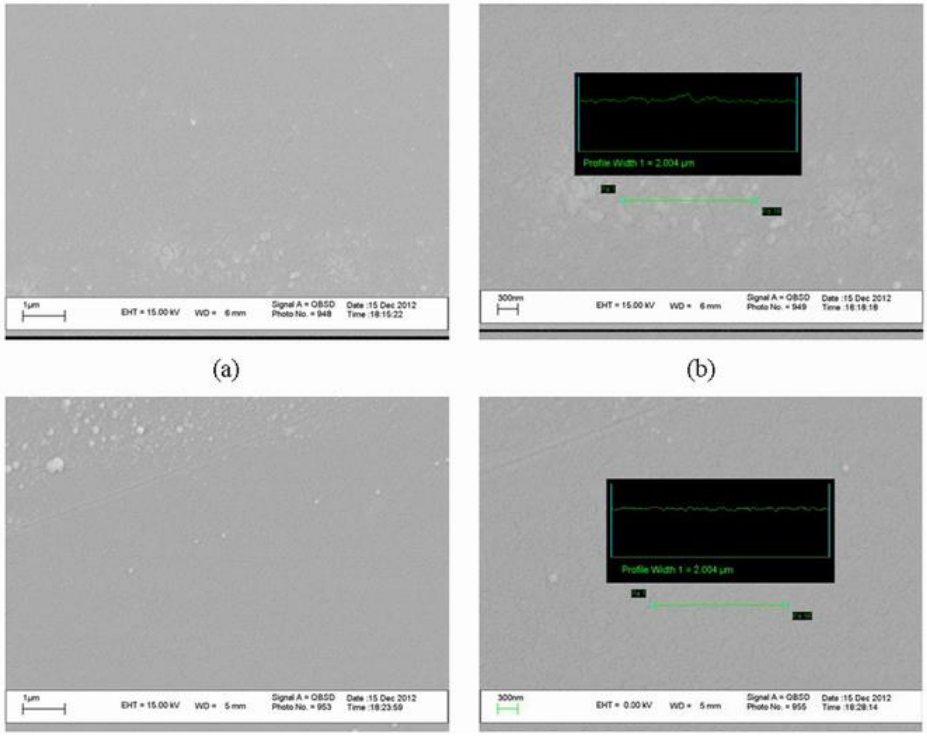


Figure 9. SEM images of the films obtained from PI (a) at 30000x and (b) at 50000x, and CPN 1% (c) at 30000x and (d) at 50000x.

4. CONCLUSION

A new thermally stable organoclay has been prepared through the treatment of Na^{+}-Mt with BAPO. XRD patterns confirmed the intercalation of organic surfactant within the silicate layers. SEM images showed that some significant changes occurred on the surface of BAPO-Mt with respect to Na^{+}-Mt, including a decrease in hydrophilicity. Furthermore, the high thermal stability of BAPO avoids pyrolysis during thermal imidization of PAA intermediate. The preparation and characterization of new PI/BAPO-Mt CPNs with different contents of organoclay have also been investigated. Nanocomposites 1-5wt.% were prepared by the thermal dehydration of a BAPO-Mt dispersion in a PAA solution obtained from BAPO and BTDA. XRD patterns showed that exfoliated CPNs may be obtained with the organoclay content of 1-3wt.%, but at higher clay loadings intercalated structure is significant. TGA-DTA and DSC measurements showed that T_g increases with increasing organoclay content loading to 1wt.%, and then decrease thereafter. SEM images showed that CPN 1wt.% produces a film with smoother surface than that of the virgin PI.

ACKNOWLEDGEMENT

The Graduate Council of the University of Mohaghegh Ardabili (Iran) is gratefully acknowledged for their financial support.

REFERENCES

ABDALLAH, W. & YILMAZER, U. 2013. Polyamide 66 nanocomposites based on organoclays treated with thermally stable phosphonium salts. *Journal of Applied Polymer Science,* 127**,** 772-783.

ARMAREGO, W. L. F. & CHAI, C. L. L. 2009. *Purification of laboratory chemicals*, Butterworth-Heinemann.

BALEK, V., BENEŠ, M., MáLEK, Z., MATUSCHEK, G., KETTRUP, A. & YARIV, S. 2006. Emanation thermal analysis study of Na-montmorillonite and montmorillonite saturated with various cations. *Journal of Thermal Analysis and Calorimetry,* 83**,** 617-623.

BATTIROLA, L. C., GASPAROTTO, L. H. S., RODRIGUES-FILHO, U. P. & TREMILIOSI-FILHO, G. 2012. Poly(imide)/Organically-Modified Montmorillonite Nanocomposite as a Potential Membrane for Alkaline Fuel Cells. *Membranes,* 2**,** 430-439.

BURNSIDE, S. D. & GIANNELIS, E. P. 1995. Synthesis and properties of new poly(dimethylsiloxane) nanocomposites. *Chemistry of materials,* 7**,** 1597-1600.

CHATZIDAKI, E. K., FAVVAS, E. P., PAPAGEORGIOU, S. K., KANELLOPOULOS, N. K. & THEOPHILOU, N. V. 2007. New polyimide–polyaniline hollow fibers: Synthesis, characterization and behavior in gas separation. *European Polymer Journal,* 43**,** 5010-5016.

DING, J., DAY, M., ROBERTSON, G. & ROOVERS, J. 2002. Synthesis and Characterization of Alternating Copolymers of Fluorene and Oxadiazole. *Macromolecules,* 35**,** 3474-3483.

EBADI, H. & MEHDIPOUR-ATAEI, S. 2010. Heat-resistant, pyridine-based polyamides containing ether and ester units with improved solubility. *Chinese Journal of Polymer Science,* 28**,** 29-37.

FUJIGAYA, T., OKAMOTO, M. & NAKASHIMA, N. 2009. Design of an assembly of pyridine-containing polybenzimidazole, carbon nanotubes and Pt nanoparticles for a fuel cell electrocatalyst with a high electrochemically active surface area. *Carbon,* 47**,** 3227-3232.

FUKASE, K., NAKAYAMA, H., KUROSAWA, M., IKEGAKI, T., KANOH, T., HASE, S. & KUSUMOTO, S. 1994. Functional Fluorescence Labeling of Carbohydrates and Its Use for Preparation of Neoglycoconjugates. *Journal of Carbohydrate Chemistry,* 13**,** 715-736.

GILMAN, J. W., JACKSON, C. L., MORGAN, A. B., HARRIS, R., MANIAS, E., GIANNELIS, E. P., WUTHENOW, M., HILTON, D. & PHILLIPS, S. H. 2000a. Flammability Properties of Polymer−Layered-Silicate Nanocomposites. Polypropylene and Polystyrene Nanocomposites. *Chemistry of materials,* 12**,** 1866-1873.

GILMAN, J. W., JACKSON, C. L., MORGAN, A. B., HARRIS, R., MANIAS, E., GIANNELIS, E. P., WUTHENOW, M., HILTON, D. & PHILLIPS, S. H. 2000b. Flammability Properties of Polymer−Layered-Silicate Nanocomposites. Polypropylene and Polystyrene Nanocomposites†. *Chemistry of materials,* 12**,** 1866-1873.

HUANG, C.-C., JANG, G.-W., CHANG, K.-C., HUNG, W.-I. & YEH, J.-M. 2008. High-performance polyimide–clay nanocomposite materials based on a dual intercalating agent system. *Polymer International,* 57**,** 605-611.

IMAI, Y., ITOYA, K., KANAMARU, M. & KAKIMOTO, M.-A. 2002. Synthesis and properties of new hydroxyl-pendant aromatic polyimides derived from trimethylsilylated 4,4′-diamino-3,3′-dihydroxybiphenyl and aromatic tetracarboxylic dianhydrides. *Journal of Polymer Science Part A: Polymer Chemistry,* 40**,** 1790-1795.

KöYTEPE, S., GURBUZ, N., ÖZDEMIR, I. & SECKIN, T. 2008. Novel Assemblies of Sn(II) Coordinated Polyimide Supported by a Ligand Containing N-Heterocyclic Phenantroline Unit. *Journal of Inorganic and Organometallic Polymers and Materials,* 18**,** 290-295.

LE, N. L., WANG, Y. & CHUNG, T.-S. 2012. Synthesis, cross-linking modifications of 6FDA-NDA/DABA polyimide membranes for ethanol dehydration via pervaporation. *Journal of Membrane Science,* 415–416**,** 109-121.

LIANG, Z.-M., YIN, J. & XU, H.-J. 2003. Polyimide/montmorillonite nanocomposites based on thermally stable, rigid-rod aromatic amine modifiers. *Polymer,* 44**,** 1391-1399.

LIAW, D.-J., LIAW, B.-Y., LI, L.-J., SILLION, B., MERCIER, R., THIRIA, R. & SEKIGUCHI, H. 1998. Synthesis and Characterization of New Soluble Polyimides from 3,3‘,4,4‘-Benzhydrol Tetracarboxylic Dianhydride and Various Diamines. *Chemistry of materials,* 10**,** 734-739.

LIU, P. 2007. Polymer modified clay minerals: A review. *Applied Clay Science,* 38**,** 64-76.

LONG, B., WANG, C.-A., LIN, W., HUANG, Y. & SUN, J. 2007. Polyacrylamide-clay nacre-like nanocomposites prepared by electrophoretic deposition. *Composites Science and Technology,* 67**,** 2770-2774.

MANSOORI, Y., AKHTARPARAST, A., REZA ZAMANLOO, M., IMANZADEH, G. & MASOOLEH, T. M. 2011a. Polymer–montmorillonite nanocomposites: Chemical grafting of polyvinyl acetate onto Cloisite 20A. *Polymer Composites,* 32**,** 1225-1234.

MANSOORI, Y., ATGHIA, S. V., SANAEI, S. S., ZAMANLOO, M. R., IMANZADEH, G. & ESKANDARI, H. 2012a. New, organo-soluble, thermally stable aromatic polyimides and poly(amide-imide) based on 2-[5-(3,5-dinitrophenyl)-1,3, 4-oxadiazole-2-yl]pyridine. *Polymer International,* 61**,** 1213-1220.

MANSOORI, Y. & DARVISHI, K. 2014. Novel Organo Soluble Polyimides and Polyimide Nanocomposites Based on 1, 4-bis ((4-aminophenyl)-1, 3, 4-oxadiazolyl) benzene, BAOB, via BAOB-modified Organoclay. *Journal of the Mexican Chemical Society,* 58**,** 126-136.

MANSOORI, Y., FATHOLLAHI, K., REZA, Z. M. & IMANZADEH, G. 2011b. Novel POBD-modified organoclay and its polyimide nanocomposites for removal of the Co(II) ion. *Polymer Composites,* 32**,** 1862-1873.

MANSOORI, Y. & GHANBARI, M. 2015. Novel polyimides obtained from a new aromatic diamine (BAPO) containing pyridine and 1,3,4-oxadiazole moieties for removal of Co(II) and Ni(II) ions. *Polymers for Advanced Technologies,* 26**,** 658-664.

MANSOORI, Y., KOHI-ZARGAR, B., SHEKAARI, H., ZAMANLOO, M. R. & IMANZADEH, G. 2012b. Synthesis of thermally stable polyamides with pendant 1,3,4-oxadiazole units via direct polycondensation in ionic liquids. *Polymer Bulletin,* 68**,** 113-139.

MANSOORI, Y. & MOHSENI MASOOLEH, T. 2015. Polyimide/organo-montmorillonite nanocomposites: A comparative study of the organoclays modified with aromatic diamines. *Polymer Composites,* 36**,** 613-622.

MANSOORI, Y. & MOHSENZADEH, R. 2015. Designed polyamides based on 1,4-bis[(4-aminophenyl)-1,3,4-oxadiazolyl]phenylene (BAPO) for removal of Cu(II) and Co(II). *Designed Monomers and Polymers,* 18**,** 333-342.

MANSOORI, Y., SANAEI, S., ZAMANLOO, M.-R., IMANZADEH, G. & ATGHIA, S. 2013. Synthesis and properties of new polyimide/clay nanocomposite films. *Bulletin of Materials Science,* 36**,** 789-798.

MANSOORI, Y., SANAEI, S. S., ATGHIA, S. V., ZAMANLOO, M. R. & IMANZADEH, G. 2011c. Synthesis of organo soluble aromatic poly(amide-imide)s based on 2-(5-(3,5-Dinitrophenyl)-1,3,4-Oxadiazole-2-YL)Pyridine in an ionic liquid. *Chinese Journal of Polymer Science (English Edition),* 29**,** 699-711.

MATSUMOTO, N., HIRUMA, H., NAGAOKA, S., FUJIYAMA, K., KANEKO, A. & KAWAKAMI, H. 2008. Cell processing on polyimide surface patterned by rubbing. *Polymers for Advanced Technologies,* 19**,** 1002-1008.

MEADOR, M. A. B., MALOW, E. J., SILVA, R., WRIGHT, S., QUADE, D., VIVOD, S. L., GUO, H., GUO, J. & CAKMAK, M. 2012. Mechanically Strong, Flexible Polyimide Aerogels Cross-Linked with Aromatic Triamine. *ACS Applied Materials & Interfaces,* 4**,** 536-544.

MEHDIPOUR-ATAEI, S. & ZIGHEIMAT, F. 2007. Soluble poly(amide imide)s containing oligoether spacers. *European Polymer Journal,* 43**,** 1020-1026.

NGUYEN, L. T. T., NGUYEN, H. N. & LA, T. H. T. 2007. Synthesis and characterization of a photosensitive polyimide precursor and its photocuring behavior for lithography applications. *Optical Materials,* 29**,** 610-618.

RINGWALD, S. C. & PEMBERTON, J. E. 1999. Adsorption Interactions of Aromatics and Heteroaromatics with Hydrated and Dehydrated Silica Surfaces by Raman and FTIR Spectroscopies. *Environmental Science & Technology,* 34**,** 259-265.

SHENG, F., TANG, X.-Z., ZHANG, S., DING, X., YU, Z.-Z. & QIU, Z. 2012. Flame retardancy of polyamide 66 nanocomposites with thermally stable organoclay. *Polymers for Advanced Technologies,* 23**,** 137-142.

SINHA RAY, S. & OKAMOTO, M. 2003. Polymer/layered silicate nanocomposites: a review from preparation to processing. *Progress in Polymer Science,* 28**,** 1539-1641.

SOUZA, F. G., SENA, M. E. & SOARES, B. G. 2004. Thermally stable conducting composites based on a carbon black-filled polyoxadiazole matrix. *Journal of Applied Polymer Science,* 93**,** 1631-1637.

TUNC, S., DUMAN, O. & KANCı, B. 2012. Rheological measurements of Na-bentonite and sepiolite particles in the presence of tetradecyltrimethylammonium bromide, sodium tetradecyl sulfonate and Brij 30 surfactants. *Colloids and Surfaces A: Physicochemical and Engineering Aspects,* 398**,** 37-47.

VAIA, R. A., VASUDEVAN, S., KRAWIEC, W., SCANLON, L. G. & GIANNELIS, E. P. 1995. New polymer electrolyte nanocomposites: Melt intercalation of poly(ethylene oxide) in mica-type silicates. *Advanced Materials,* 7**,** 154-156.

VOEVODIN, A. A., O'NEILL, J. P. & ZABINSKI, J. S. 1999. Nanocomposite tribological coatings for aerospace applications. *Surface and Coatings Technology,* 116–119**,** 36-45.

WANG, H.-W., DONG, R.-X., LIU, C.-L. & CHANG, H.-Y. 2007a. Effect of clay on properties of polyimide-clay nanocomposites. *Journal of Applied Polymer Science,* 104**,** 318-324.

WANG, J., IROH, J. O. & LONG, A. 2012. Controlling the structure and rheology of polyimide/nanoclay composites by condensation polymerization. *Journal of Applied Polymer Science,* 125**,** E486-E494.

WANG, S.-F., LIN, M.-L., SHIEH, Y.-N., WANG, Y.-R. & WANG, S.-J. 2007b. Organic modification of synthesized clay-magadiite. *Ceramics International,* 33**,** 681-685.

WANG, X., LI, Y., GONG, C., MA, T. & ZHANG, S. 2009. Synthesis and properties of new poly(ether imides) based on pyridine-containing aromatic dianhydride and diamine monomers. *Journal of Applied Polymer Science,* 113**,** 1438-1447.

YEH, J.-M., CHEN, C.-L., KUO, T.-H., SU, W.-F., HUANG, H.-Y., LIAW, D.-J., LU, H.-Y., LIU, C.-F. & YU, Y.-H. 2004a. Preparation and properties of (BATB–ODPA) polyimide–clay nanocomposite materials. *Journal of Applied Polymer Science,* 92**,** 1072-1079.

YEH, J.-M., LIOU, S.-J. & CHANG, Y.-W. 2004b. Polyacrylamide–clay nanocomposite materials prepared by photopolymerization with acrylamide as an intercalating agent. *Journal of Applied Polymer Science,* 91**,** 3489-3496.

YEUM, J. H. 2011. Novel Poly(vinyl alcohol)/Clay Nanocomposite Microspheres via Suspension Polymerization and Saponification. *Polymer-Plastics Technology and Engineering,* 50**,** 1149-1154.

YOKOYAMA, R., SUZUKI, S., SHIRAI, K., YAMAUCHI, T., TSUBOKAWA, N. & TSUCHIMOCHI, M. 2006. Preparation and properties of biocompatible polymer-grafted silica nanoparticle. *European Polymer Journal*, 42**,** 3221-3229.

YOONESSI, M., SHI, Y., SCHEIMAN, D. A., LEBRON-COLON, M., TIGELAAR, D. M., WEISS, R. A. & MEADOR, M. A. 2012. Graphene Polyimide Nanocomposites; Thermal, Mechanical, and High-Temperature Shape Memory Effects. *ACS Nano,* 6**,** 7644-7655.

YOUSFI, M., SOULESTIN, J., VERGNES, B., LACRAMPE, M. F. & KRAWCZAK, P. 2013. Morphology and mechanical properties of PET/PE blends compatibilized by nanoclays: Effect of thermal stability of nanofiller organic modifier. *Journal of Applied Polymer Science,* 128**,** 2766-2778.

ZHONG, Y., JANES, D., ZHENG, Y., HETZER, M. & DE KEE, D. 2007. Mechanical and oxygen barrier properties of organoclay-polyethylene nanocomposite films. *Polymer Engineering & Science,* 47**,** 1101-1107.

ZIDELKHEIR, B. & ABDELGOAD, M. 2008. Effect of surfactant agent upon the structure of montmorillonite. *Journal of Thermal Analysis and Calorimetry,* 94**,** 181-187.